J. Fluid Mech. (1990), *vol.* 221, *pp.* 577–596
Printed in Great Britain

Measurement of the average velocity of sedimentation in a dilute polydisperse suspension of spheres

By D. BRUNEAU[1], R. ANTHORE[2], F. FEUILLEBOIS[1], X. AUVRAY[2] AND C. PETIPAS[2]

[1] Laboratoire d'Aérothermique du CNRS, 4 ter, route des Gardes, F-92190 Meudon, France

[2] Laboratoire des Rayons X, URA 808, Faculté des Sciences et Techniques, Université de Rouen, BP 118, 76134 Mont Saint Aignan, France

(Received 5 September 1989 and in revised form 17 May 1990)

An X-ray attenuation technique is used to obtain the local concentration of spherical particles in a polydisperse suspension as a function of vertical position and time. From these experimental data, the average velocity of sedimentation in the homogeneous part of the suspension is derived by considering the variation with time of the total volume of particles located above a given fixed horizontal plane. Measurements have been performed in suspensions of particles which differ from each other in size with a total volume concentration in particles between 0.13% and 2.5%, and also in suspensions of particles which differ from each other both in size and in density, the total volume concentration being 2%. For the first kind of suspension, the experimental hindered settling factor is plotted versus the concentration and a linear regression analysis provides the slope with its 90% confidence limits: $S_e = -5.3 \pm 1.1$. This experimental average coefficient of sedimentation is in good agreement with the theoretical average coefficient $S_t = -5.60$ obtained from the results of Batchelor & Wen (1982). The second kind of suspension, for which permanent doublets of spheres may theoretically exist, is not in the range of validity of Batchelor & Wen's results. The experimental average coefficient of sedimentation for this case is found to be much larger than the prediction obtained by extrapolating Batchelor & Wen's results out of their range of validity. This increased velocity may be experimental evidence of the existence of permanent doublets.

1. Introduction

The sedimentation of solid particles in a viscous fluid is a common industrial process in civil, chemical and oil engineering. Various applications are the sifting of particles with different sedimentation velocities, and the separation of particles from a fluid by decantation. Many theoretical and experimental works have been published during the last twenty years on this subject. On the theoretical side, Batchelor (1982) showed that the average velocity V_i of a test particle of type i settling in a dilute homogeneous polydisperse suspension made of N different types of sphere has the form:

$$V_i = U_{i,0}\left(1 + \sum_{j=1}^{N} S_{ij}\,\phi_{j0}\right), \tag{1}$$

$\lambda\backslash\gamma$	-2	-1	-0.5	0	0.6	1	1.5	2.25
0.25	-1.96	-2	-2.2	-2.56	-3.31	-3.83	-4.73	-6.9
0.5	-2.51	-2.27	-2.28	-2.53	-3.41	-4.29	-6.77	—
1				$S_{ij} = -2.52 - 0.13\gamma$ $(\gamma \neq 1)$				
2	3.18	-0.34	-1.89	-2.44	-9.85	-9.81	-11.16	-13.71
4	26.63	10.05	2.03	-2.66	-19.55	-24.32	-32.71	—

TABLE 1. Calculated values of the sedimentation coefficient S_{ij} for negligible Brownian effect and interparticle forces, and for different values of λ and γ (after Batchelor & Wen 1982).

λ	0.125	0.25	0.5	0.9	1.1	2	4	8
S_{ij}	-3.68	-3.83	-4.29	-5.29	-5.95	-9.81	-24.32	-78.53

TABLE 2. Calculated values of S_{ij} for negligible Brownian effect and interparticle forces, for $\gamma = 1$ and for different values of λ (after Batchelor & Wen 1982).

where $U_{i,0}$ is the velocity of a i-particle when falling in isolation (Stokes 1851)

$$U_{i,1} = \frac{2g}{9\eta} a_i^2 (\rho_i - \rho), \tag{2}$$

ϕ_{j0} is the volume concentration in spheres of type j, and S_{ij} is the dimensionless sedimentation coefficient which depends on the radius ratio $\lambda = a_j/a_i$, the reduced density ratio $\gamma = (\rho_j - \rho)/(\rho_i - \rho)$, a dimensionless quantity taking into account the interparticle force potential (i.e. the van der Waals and electrostatic forces), and the Péclet number linked to the relative motion of an i-particle and a j-particle,

$$\mathbb{P}_{ij} = \frac{2\pi g}{3kT_e} a_i^4 (\rho_i - \rho)\, \lambda |\gamma\lambda^2 - 1|, \tag{3}$$

which evaluates the relative importance of the gravity effect and Brownian motion effect. In these equations, the quantities a_i, ρ_i, ρ, η, g, k and T_e are respectively the radius of an i-particle, the density of an i-particle, the density and the dynamic viscosity of the fluid, the body force per unit mass, the Boltzman constant and the absolute temperature of the suspension. Values of the sedimentation coefficient have been computed by Batchelor & Wen (1982) for, among other results, negligible Brownian effect and interparticle forces (tables 1 and 2). As Batchelor & Wen wrote in 1982, there are combinations of values of λ and γ for which some relative trajectories of the two particles may either be of finite length or have the form of a closed periodic orbit (see Wacholder & Sather 1974). For these values, they could not determine the pair distribution function $n_j p_{ij}(\boldsymbol{r})$ (in Batchelor's notation, n_j being the number of particles j per unit volume) defined as the probability of finding the centre of a j-particle in unit volume at position $\boldsymbol{r}$ relative to the centre of an i-particle. This is because the boundary condition $p_{ij}(\boldsymbol{r}) \to 1$ when $|\boldsymbol{r}| \to \infty$ could not be applied ($\boldsymbol{r}$ is always finite). Thus S_{ij} could not be calculated (hence the dashes in table 1 and also some gaps between the calculated values shown in table 1).

Kops-Werkhoven & Fijnaut (1981) measured the velocity of sedimentation of monodisperse Brownian particles 0.04 μm in diameter and found the coefficient of sedimentation $S_{ii} = -6 \pm 1$ consistent with Batchelor's (1972) theoretical result $S_{ii} = -6.55$.

In our article, we will only consider the case of non-Brownian particles. There appears to be no experimental data which can be compared with the theory of Batchelor (1982) which is valid only for dilute and homogeneous suspensions. Mirza & Richardson (1979) measured visually the velocity of the top of the particle cloud, the total volume concentration ϕ_0 being between 25% and 45%. Ham & Homsy (1988) examined the motion of an individual sphere settling in a monodisperse suspension, the total volume concentration ϕ_0 being in the range 2.5%–10%. All particles, except the one observed, were made transparent by matching the index of refraction of the fluid. They recorded the arrival times of the test sphere at successive horizontal planes and they derived from these data the average velocity of the sphere between these planes. They found a $1-4\phi_0+8\phi_0^2$ dependence of the settling speed on the volume concentration. The relative error on their data was about 10%. Davis & Hassen (1988) obtained, through a light-sheet attenuation process, the evolution in time of the particle volume concentration in four different horizontal planes, for suspensions with total volume concentrations, ϕ_0, in the range 0.1%–15%. From these data, they calculated the median velocity of the spreading interface situated between the clarified fluid and the homogeneous part of the suspension (this non-homogeneous part of the suspension is called the top front) and also the spreading rate of this interface. Davis & Birdsell (1988) used the same light-sheet attenuation principle to measure the median velocity of the above-mentioned non-homogeneous interface for mixtures of three different sets of particles, each set being characterized by a density and a median particle diameter. They compare this velocity with the average velocity of sedimentation valid for homogeneous and dilute suspensions obtained from the results of Batchelor & Wen. Bacri *et al.* (1986) followed, by means of an acoustic technique, the time and space dependence of the concentration of a settling suspension composed of spherical glass spheres in water, the total volume concentrations ϕ_0 being larger than 20%.

Our objective is to obtain an experimental average velocity of sedimentation in the homogeneous part of the suspension in order to compare it to the 'exact' results (valid for homogeneous and dilute suspensions) of Batchelor (1982) and Batchelor & Wen (1982). For that purpose, we obtained, by means of an X-ray attenuation technique, the particle volume concentration as a function of the vertical position in the measurement cell for different successive times (see §2). The experimental system used is an improved version of the apparatus already used by Anselmet *et al.* (1989), Aïdi (1986), Aïdi *et al.* (1989).

The next section is devoted to a description of the experimental apparatus and procedure. The method of data analysis is then explained in §3. Section 4 contains the experimental results obtained for the average coefficients of sedimentation and the comparison of these results with the theory. Finally, the conclusion is in §5.

2. Experimental system and procedure

2.1. *Experimental set-up*

The experimental set-up is shown in figure 1(*a*). X-rays generated by the source S are diffracted by a quartz monochromator M so as to obtain a monochromatic beam. The X-rays then pass through a nickel filter F_1. Three slots F_1, F_2, F_3 eliminate the parasitic rays and a void enclosure V eliminates the air absorption on the way to the measurement cell C. The photons coming out of the cell are collected on a linear localization detector D standing close to the cell. The resulting electric output signal from the detector is converted and recorded in a multichannel analyser A, and then

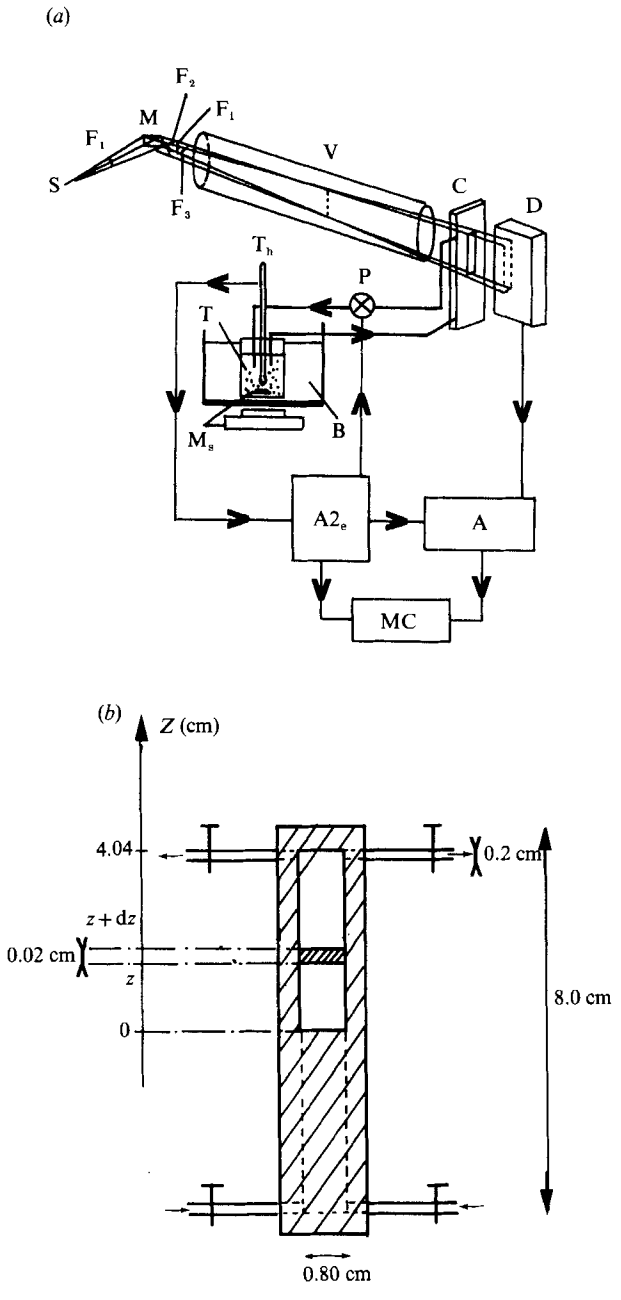

FIGURE 1. Schematic diagram. (*a*) Experimental apparatus. (*b*) Arrangement of the measurement cell.

treated on a microcomputer MC under the UNIX system. The measurement cell is connected to a tank T where a mixture of particles in a fluid is kept homogeneous by a magnetic stirrer M_s and stabilized in temperature by a heat-controlled bath B. This temperature is measured in the tank with a platinum resistance thermometer T_h. Before each new experiment, the cell is then filled up by a peristaltic pumping system P. This whole system, including the data acquisition, is driven by a

microcomputer Apple 2e denoted by $A2_e$ in figure 1. This experimental system provides the time evolution of the transmitted X-ray intensity through the cell versus the height z in the cell.

The source of X-rays is a tube with a copper anode. The voltage applied to the tube target is low enough not to excite harmonics ($\frac{1}{2}\lambda$). As the beam comes out of the slots, it is 5.00 cm high and 0.60 cm wide.

The measurement cell is represented in more detail in figure 1 (*b*). It is 8.00 cm high, 0.80 cm wide and 1.06 cm thick and is divided into two parts: the top part is made of a 4.04 cm high window transparent to X-rays and the bottom part is used only for the particles to settle. Hereafter, the origin of the vertical position $z = 0$ in the cell is the bottom of the window. Before each sedimentation run, the suspension circulates through the cell, entering the cell by two horizontal pipes located in its lower part, and leaving it by two more horizontal pipes located in its upper part. The circulation is activated by two peristaltic pumps. The rotors of the pumps are out of phase in order to avoid any pulsating flow. As soon as the peristaltic pumps are stopped, actuator valves in the four pipes close and thus no residual circulation between the tank and the cell is possible. Furthermore, in order to avoid the effects of convection within the cell arising from heat transfer to the surroundings, the temperature of the cell is stabilized by the heat-controlled bath B (for clarity, the tubes which permit the circulation of the heat-controlled fluid B around the cell have not been represented in the figures 1*a* and 1*b*).

The linear localization detector, which gives a signal proportional to the received energy, allows 7000 X-photons per second to be located vertically with a spatial resolution $dz = 200$ μm.

2.2. *Particles and fluid*

The system of particles and the fluid used in the experiment were chosen according to several criteria. First, the Reynolds number of each particle

$$\mathbb{R}_i = \frac{\rho U_{i,0} a_i}{\eta}, \tag{4}$$

has to be small for our experimental conditions to be compatible with the assumptions of the theory of Batchelor (1982). Thus the particles have to be small enough, and the fluid viscosity large enough. Secondly, the absorption coefficients of the fluid and the particles have to be different enough so that the contrast is sufficient to measure the attenuation of the X-ray beam due to the particles. Finally, we choose to study the case of a large Péclet number relative to each particle (that is non-Brownian particles)

$$\mathbb{P}_i = \frac{4\pi g}{3kT_e} a_i^4(\rho_i - \rho), \tag{5}$$

so that the Péclet number for the relative motion of two particles (equation (3)) is generally also large. Thus, the particles have to be typically larger than 1 μm and their densities have to be significantly different from the fluid density.

A set of spheres having a given medium size, manufactured with a given material always presents a dispersion in densities and a dispersion in diameters which depend on the fabrication process. In fact, the dispersion in densities is negligible compared to the dispersion in diameters. Thus, every set of spheres is characterized by a density, an absorption coefficient and a discrete histogram of diameters which is obtained with an image processing technique. This technique is based on the surface

(*a*) $2a_i$ (μm)	Number fraction	(*b*) $2a_i$ (μm)	Number fraction
94	0.073	140	0.001
98	0.225	148	0.003
102	0.230	156	0.022
106	0.178	164	0.079
110	0.168	172	0.185
114	0.058	180	0.155
118	0.042	188	0.182
122	0.026	196	0.169
		204	0.136
		212	0.038
		220	0.007
		228	0.004
		236	0.004
		244	0.003
		252	0.001
		260	0.001
		268	0.006
		276	0.002
		284	0.003

TABLE 3. (*a*) Discrete diameter histogram of the set of silica spheres. (*b*) Discrete diameter histogram of the set of magnesium spheres.

measurement of the shadow of an illuminated particle (that is the surface measurement of the perpendicular projection of a particle on a horizontal plane). This has been done with a Leitz TAS Analyser equipped with a Plunbicon camera which has been especially selected by the manufacturer (the camera is rectified in astigmatism and in grey level). The relative error on this surface measurement is less than 4% because of the very good contrast and thus the precision on the measurement of a particle radius is better than 2%. Two sets of particles have been prepared by sifting, one with silica (density 2550 kg/m^3) and one with magnesium (density 1745 kg/m^3); obviously, there is a limited number of materials with the required absorption coefficient and for which non-Brownian spheres are available. For each set of particles, more than 1500 particles have been analysed. The error in measuring the average diameter of each set is less than 0.4% (see Coster & Chermant 1989). The particles in each set were then classified in histograms in different ways as follows. For silica, the median diameters of the classes were:

(i) 94, 98, 102, ..., 122 μm,
(ii) 94, 97, 100, ..., 121 μm,
(iii) 94, 96, 98, ..., 122 μm,
(iv) 93, 95, 97, ..., 121 μm.

For magnesium, the median diameters of the classes were:

(i) 140, 148, 156, ..., 284 μm,
(ii) 140, 144, 148, ..., 284 μm,
(iii) 140, 142, 144, ..., 284 μm.

For example, the discrete diameter histograms '(i)' for silica and magnesium are respectively given in table 3(*a*, *b*).

The experiments were carried out in a fluid which is a mixture of 25% volume of glycerol and 75% isopropanol. Its density and its kinematic viscosity, at $T_e = 293.5$ K, are respectively $\rho = 915$ kg/m^3 and $\nu = 1.322 \times 10^{-5}$ m^2/s.

2.3. *Experimental procedure and discussion of the initial conditions*

Each mixing process consisted of filling up the cleaned tank with a known quantity of fluid and then adding enough magnesium and silica spheres (in volume concentrations ϕ_{0m}, ϕ_{0s}, respectively) in order to obtain a required total volume concentration

$$\phi_0 = \phi_{0m} + \phi_{0s}, \tag{6}$$

and a required magnesium spheres/silica spheres volume proportion

$$p_0 = \frac{\phi_{0m}}{\phi_0} = \frac{\phi_0 - \phi_{0s}}{\phi_0}. \tag{7}$$

The first step in the experimental procedure is to measure the intensity I_f of the X-ray beam at the input of the detector, the cell being filled up with the particle-free fluid. This is done by recording the output data from the detector during an accumulating time t_a of half an hour. This result provides us with a reference value for the transmitted intensities, to be used later in the data analysis explained in §3. A full experiment is then carried out following several steps: first, the diphasic mixture is homogenized by the magnetic stirrer. Then, the peristaltic pumps circulate the mixture between the tank and the cell for 30 s. Finally the circulation is stopped and the actuator valves are closed. The particles which are then in the horizontal pipes generally settle down towards the wall of the pipes although a negligible number of particles might settle outside the tubes feeding the top of the cell. It is also observed visually that the residual turbulence within the cell does not persist more than one second after the circulation is stopped.

One might wonder whether the initial circulation might induce a peculiar distribution of particles and distribution of pairs of particles in the suspension.

We can evaluate the influence of the fluid inertia as a possible segregating agent during the initial circulation. The flow in the cell is then a Poiseuille flow with maximum velocity $u_m \approx 0.04$ m/s. Using Vasseur & Cox's results (1976), we calculate the migration velocity w_i of an i-sphere due to fluid inertia in a Poiseuille flow between two parallel walls

$$w_i = u_m \mathbb{R}_i K, \tag{8}$$

where the Reynolds number (defined in equation (4)) is around 0.13 for the largest particles and K, varying across the cell, is at most $|K| = 0.04$. We obtain $w_i = 2 \times 10^{-4}$ m/s for the largest particles and $w_i = 2 \times 10^{-5}$ m/s on average for the particles we use in our suspension. Thus, the horizontal inertial migration distance of the particles during their motion through the cell (at most 4×10^{-4} m and in average 4×10^{-5} m) is too small to create a non-homogeneous particle distribution characteristic of a tubular pinch effect.

Because of the circulation of the suspension through the cell before each experiment, the statistical structure of the suspension initially present in the cell (that is the pair distribution function $n_j p_{ij}(\boldsymbol{r})$ when only interactions between two particles are taken into account) is that corresponding to the Poiseuille flow; Nevertheless, the structure of the suspension evolves rapidly from that due to the Poiseuille flow to that due to the settling. This may be seen from the equation for the pair distribution function valid for large Péclet numbers $\mathbb{P}_{ij}$ (Batchelor 1982)

$$\frac{\partial p_{ij}(\boldsymbol{r})}{\partial t} + \nabla \cdot (V_{ij}\, p_{ij}(\boldsymbol{r})) = 0, \tag{9}$$

where
$$V_{ij} = U_{j,0} - U_{i,0}. \tag{10}$$

A characteristic time of this equation, that is a characteristic time for the evolution of the statistical structure of the suspension is

$$\tau = \frac{a}{V_{ij}} \approx \frac{a}{(2g/9\eta)(a_j^2 - a_i^2)(\rho_p - \rho)} \approx \frac{a^2}{2\Delta a}\frac{1}{U_0}, \tag{11}$$

where a, ρ_p, U_0 are the mean radius, the mean density, the mean Stokes velocity of the particles and $\Delta a = a_j - a_i$. A characteristic distance covered by the two considered particles during the time τ is

$$d = \tau U_0 = \frac{a^2}{2\Delta a}. \tag{12}$$

For example, for $a_j = 100$ μm and $a_i = 95$ μm, $\tau = 1.3$ s and $d = 0.09$ cm. Thus, except for pairs of spheres with nearly equal sizes (the effect of which is not essential in the calculation of the average coefficient of sedimentation as explained at the end of §4), the distance for which the structure of the suspension evolves from that due to the Poiseuille flow to that due to settling is much smaller than the total observed sedimentation distance (4.04 cm).

As an independent check of the homogeneity of the concentration and pair distribution function along a horizontal plane, measurements of the volume concentration in particles have been made in several vertical slices of the cell with an X-ray beam less than 0.1 cm large. The concentration obtained from these measurements (by the procedure explained in §3) was found to be identical in these vertical slices.

To conclude on the question of the initial conditions, we consider that at a time $t_v = 1$ s after the circulation is stopped, the mixture is homogeneous and the sedimentation really begins. Moreover, it will be seen in the section on data analysis that the way to obtain the hindered settling factor from the experimental data does not depend on the data recorded during the first few seconds after the circulation is stopped (cf. the explanations about the straight parts of the curves in figure 3).

During the sedimentation, N_r recordings are taken out, each of them being characterized by an accumulating time t_{a_i} ($i = 1, 2, \ldots, N_r$); they are separated from each other by a time Δt_i ($i = 1, 2, \ldots, N_r - 1$). Every time the detector locates an X-photon during the ith recording, a pulse is sent to the ith absorption spectrum on the multichannel analyser, in the channel corresponding to the height in the cell where it was located. At the end of the ith recording, each channel of the ith absorption spectrum contains the number of photons which arrived on the detector at the corresponding height during the accumulation time t_{a_i} (the number of photons per unit time is proportional to the transmitted intensity). Such an experiment is carried out several times (about a hundred times), the circulation of the diphasic mixture being reset before each new experiment, in order to ensure accurate experimental data for the time evolution of the transmitted intensity through the cell versus the height z in the cell. We now define the sedimentation time t_{s_i} ($i = 1, 2, \ldots, N_r$) as the time between the vanishing of the residual turbulence within the cell (after the circulation is stopped) and the middle of the ith recording; therefore, this time is given by the next equation:

$$t_{s_i} = \sum_{k=1}^{i-1} (t_{a_k} + \Delta t_k) + \tfrac{1}{2} t_{a_i} - t_v. \tag{13}$$

with the convention that the sum is zero if $i = 1$.

3. Data analysis

The purpose of this section is to obtain, from the experimental data mentioned in §2, the volume concentration as a function of the height in the measurement cell, for different sedimentation times, and then an average velocity of sedimentation in the homogeneous part of the suspension. In order to obtain the volume concentration, we first write the classical exponential decay law (Klug & Alexander, 1954) for the intensity of X-rays I_f transmitted through the cell filled up with particle-free fluid:

$$I_f = I_0 \exp(-\alpha_f l), \tag{14}$$

where I_0 is the X-ray intensity falling on the cell, α_f the linear absorption coefficient of the fluid and l the thickness of the cell. In the same way, we write $I(t_s, z)$ the intensity transmitted through the cell filled with the settling suspension of particles in a fluid

$$I(t_s, z) = I_0 \exp\left[-\sum_{i=1}^{N} \alpha_i l_i(t_s, z) - \alpha_f \left(l - \sum_{i=1}^{N} l_i(t_s, z)\right)\right] \tag{15}$$

where α_i is the linear absorption coefficient of an i-particle, $l_i(t_s, z)$ is the total equivalent thickness of i-particles crossed by the X-ray beam and N is the number of types of particles in the suspension. This intensity has been obtained experimentally with a very fine spatial and temporal resolution and is thus considered here as a continuous function of z and t_s. Combining (14) and (15) along with the definition of the transmission factor

$$T(t_s, z) = \frac{I(t_s, z)}{I_f}, \tag{16}$$

yields

$$T(t_s, z) = \exp\left(-\sum_{i=1}^{N} k_i \phi_i(t_s, z)\right), \tag{17}$$

with

$$k_i = (\alpha_i - \alpha_f) l, \tag{18}$$

and

$$\phi_i(t_s, z) = \frac{l_i(t_s, z)}{l}, \tag{19}$$

which is in fact the volume concentration in i-particles.

Let us now define

$$\phi(t_s, z) = \phi_0 \frac{\ln T(t_s, z)}{\ln T_0}, \tag{20}$$

which has the dimension of a volume concentration. ϕ_0, the initial total volume concentration, and T_0, the initial transmission factor, are independent of z. This definition, combined with (17), yields

$$\phi(t_s, z) = \phi_0 \frac{\sum_{i=1}^{N} k_i \phi_i(t_s, z)}{\sum_{i=1}^{N} k_i \phi_{i0}}, \tag{21}$$

where ϕ_{i0}, the initial value of the volume concentration $\phi_i(t_s, z)$ of i-particles, is independent of z. For suspensions in which we find only one particle set, that is particles made of a given material (silica or magnesium), the attenuation coefficients α_i are all the same and (21) shows that $\phi(t_s, z)$ is effectively the total volume concentration in particles.

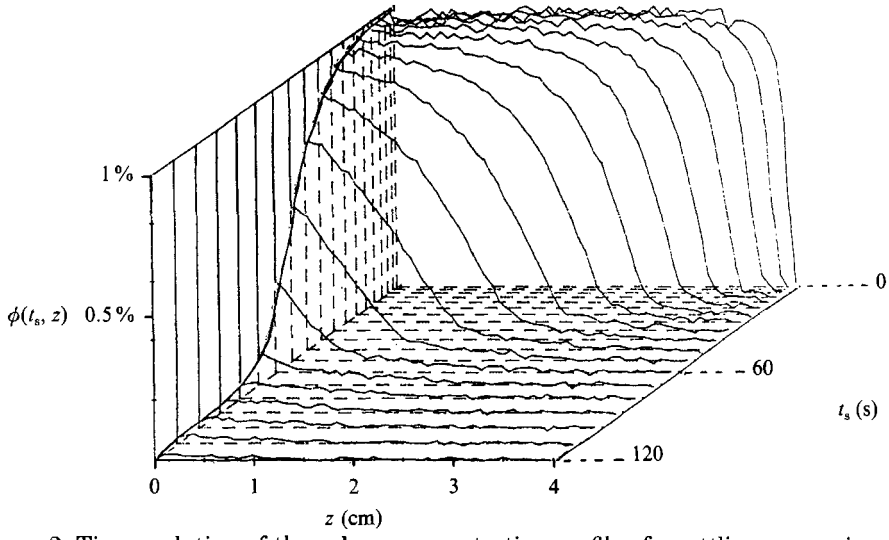

FIGURE 2. Time evolution of the volume concentration profile of a settling suspension of silica spheres ($\phi_0 = 1\,\%$, $p_0 = 0$).

The X-ray attenuation technique is calibrated in the following way. The initial transmitted intensity through the homogeneous part of a suspension of a given material, say silica, is measured for various values of the volume concentration ϕ_0. The reference transmitted intensity, I_t, is measured systematically as explained in the preceding section. The initial transmission factor T_0 obtained from (16) is related to ϕ_0 by (17) where $k_i = k_{\mathrm{Si}}$, the attenuation coefficient for silica:

$$\ln T_0 = -k_{\mathrm{Si}}\,\phi_0. \tag{22}$$

The linearity of $\ln T_0$ with respect to ϕ_0 is verified by calculating the least-squares linear regression line. The slope of this line provides us with an accurate value of the coefficient k_{Si}. The determination of k_{Mg} for magnesium proceeds along the same lines. Using this procedure, we found:

$$k_{\mathrm{Si}} = 1.32, \quad k_{\mathrm{Mg}} = 0.85. \tag{23}$$

Let us now return to the analysis of the measurement data in the general case of a mixture of silica and magnesium spheres. Once I_t, ϕ_0 and T_0 are known, the measured intensity profiles $I(t_s, z)$ give the function $\phi(t_s, z)$ by (16) and (20). Figure 2 shows an example of the time evolution of the volume concentration profile $\phi(t_s, z)$ for a settling suspension of silica spheres ($\phi_0 = 1\,\%$, $p_0 = 0$) with $N_r = 60$, $\Delta t_i = 0$, $t_{a_i} = 0.3125(7+i)$ s. At a given 'control plane' $z = z_p$, the volume concentration of particles remains constant at a value equal to the bulk concentration for a certain period of time. Then the non-homogeneous part of the particle cloud, called the top front, passes through this plane $z = z_p$, the volume concentration falling to zero (the fluid is then free from particles above the plane $z = z_p$). Furthermore, the spreading of the top front can be roughly observed on figure 2: the top front is initially of zero thickness and then grows rapidly. Note that Davis & Hassen (1988) observed a slower growth of the top front. However, this may be because our silica spheres have a wide diameter histogram compared with those of Davis & Hassen.

Once the profile $\phi(t_s, z)$ is known, a characteristic volume $V_{z_p}(t_s)$ can be calculated in the following way

$$V_{z_p}(t_s) = A \int_{z_p}^{H} \phi(t_s, z)\,\mathrm{d}z, \tag{24}$$

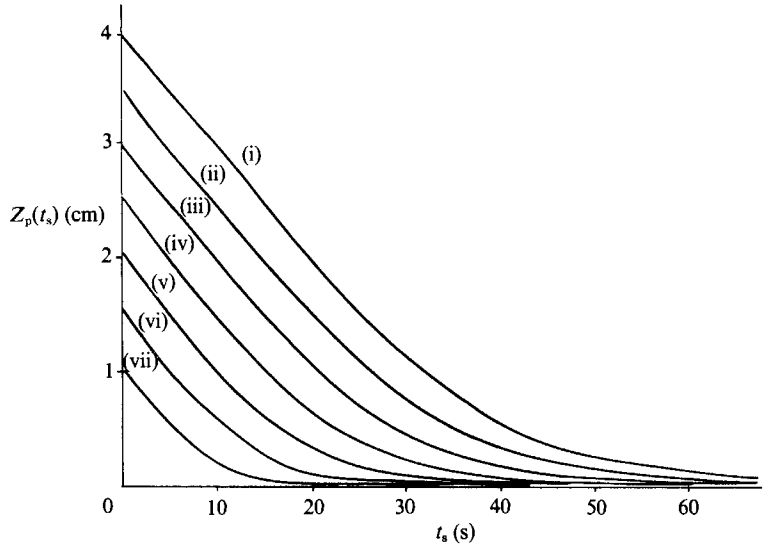

FIGURE 3. Reduced volume $Z_p(t_s)$, for different control planes, of a settling suspension of magnesium spheres and silica spheres ($\phi_0 = 2\%$, $p_0 = 0.75$). (i) $z = 0.04$ cm; (ii) $z = 0.54$ cm; (iii) $z = 1.04$ cm; (iv) $z = 1.54$ cm; (v) $z = 2.04$ cm; (vi) 2.54 cm; (viii) $z = 3.04$ cm.

where $H = 4.04$ cm is the top of the window of the measurement cell and A is the area of the cross-section of the measurement cell. For a suspension of particles made of the same material, $V_{z_p}(t_s)$ is simply the volume of particles located between $z = z_p$ and $z = H$.

In order to use the formalism derived so far to obtain the average velocity of sedimentation, it is useful to plot a quantity which has the dimension of a length, namely the reduced volume $Z_p(t_s) = V_{z_p}(t_s)/A\phi_0$ as a function of t_s. This reduced volume can be written in the following form (see equations (21) and (24)):

$$Z_p(t_s) = \frac{1}{\sum_{i=1}^{N} k_i \phi_{i0}} \sum_{i=1}^{N} k_i \int_{z_p}^{H} \phi_i(t_s, z)\, dz. \tag{25}$$

For particles made of a given material, the reduced volume $Z_p(t_s)$ would represent the height of the part of the suspension above $z = z_p$ if that part were homogeneous (with concentration ϕ_0), that is if the top front had zero width. As an example, the curve of $Z_p(t_s)$, for different control planes $z = z_p$, in a settling suspension of magnesium spheres and silica spheres ($\phi_0 = 2\%$, $p_0 = 0.75$) with $N_r = 60$, $\Delta t_i = 0$ and $t_{a_i} = 0.3125\ (7+i)$ s, is shown in figure 3. Note that for a given control plane, part of the curve is a straight line. This corresponds to the homogeneous part of the suspension, having concentrations $\phi_i(t_s, z)$ equal to the initial concentrations ϕ_{i0} ($i = 1, 2, \ldots, N$), passing through this plane. The trailing part of the curve to zero corresponds to the top front passing through this plane.

An experimental average velocity V of sedimentation in the homogeneous part of the suspension can now be defined by considering the derivative of $Z_p(t_s)$ with respect to the sedimentation time t_s, that is the slope of the straight part of the curves shown in figure 3 (V is equal to the flux of $Z_p(t_s)$ through the plane $z = z_p$)

$$V = \frac{d}{dt_s} Z_p(t_s). \tag{26}$$

The flux of i-particles across the plane $z = z_p$ located in the homogeneous part of the suspension is equal to the variation in time of the volume of particles located above that plane

$$\phi_{i0} V_i = \frac{\mathrm{d}}{\mathrm{d}t_s} \int_{z_p}^{H} \phi_i(t_s, z)\, \mathrm{d}z, \tag{27}$$

where V_i is the velocity of a i-particle in the homogeneous part of the suspension. Then from (26), (25) and (27) an expression of the experimental average velocity V is

$$V = \frac{\sum_{i=1}^{N} k_i \phi_{i0} V_i}{\sum_{i=1}^{N} k_i \phi_{i0}}. \tag{28}$$

For suspensions of particles made of the same material, the velocity V is simply the mean of the velocities V_i of all types of particles weighted with the volume concentrations ϕ_{i0}.

This expression (28) of the experimental average velocity provides the link for the comparison with the theory. By introducing the theoretical expression for the average velocity V_i of each type i of particles ((1) and (2)) in (28), we obtain:

$$V = U(1 + S_t \phi_0), \tag{29}$$

with

$$U = \frac{\phi_0}{\sum_{i=1}^{N} k_i \phi_{i0}} \frac{2g}{9\eta} \sum_{i=1}^{N} k_i \chi_{i0} a_i^2 (\rho_i - \rho), \tag{30}$$

$$S_t = \frac{\sum_{i=1}^{N} k_i \chi_{i0} a_i^2 (\rho_i - \rho) \sum_{j=1}^{N} S_{ij} \chi_{j0}}{\sum_{i=1}^{N} k_i \chi_{i0} a_i^2 (\rho_i - \rho)}, \tag{31}$$

where $\chi_{i0} = \phi_{i0}/\phi_0$ is the volume fraction of particles i. U is there an average Stokes velocity weighted with the k_i coefficients (obtained from the calibration) and the initial volume proportions χ_{i0}. Note that the Stokes velocities (which are proportional to $a_i^2(\rho_i - \rho)$) also contribute to the theoretical average coefficient of sedimentation S_t.

When the two particles i and j differ from each other in size and (or) density, the values of S_{ij} are obtained by interpolating from table 1. More values are given in table 2 for when the two particles differ in size only. These values are correct if the particles i and j considered are very different, since, for nearly identical particles (that is $\lambda \to 1$ and $\gamma \to 1$), the theoretical coefficient S_{ij} calculated by Batchelor (1972, 1982) shows a singular theoretical behaviour. As a matter of fact, the value of S_{ij}, when it is known, depends on how γ and λ tend towards the limit value 1:

(i) for $\lambda = \gamma = 1$, that is $\mathbb{P}_{ij} = 0$, Batchelor (1972) obtained, taking into account the Brownian effect, $S_{ii} = -6.55$,

(ii) for $\gamma = 1$ and $\lambda \to 1$, by extrapolating the coefficient S_{ij} from those given in table 2 ($\gamma = 1$, $\lambda \neq 1$, $\mathbb{P}_{ij} \gg 1$), $S_{ii} \approx -5.6$,

(iii) for $\lambda = 1$ and $\gamma \to 1$, by extrapolating the coefficient S_{ij} from those given in table 1 ($\lambda = 1$, $\gamma \neq 1$, $\mathbb{P}_{ij} \gg 1$), $S_{ii} \approx -2.65$,

(iv) for $\lambda \to 1$ and $\gamma \to 1$ simultaneously, the value of S_{ii} remains unknown.

This singular theoretical behaviour, can be explained as follows: the Péclet number $\mathbb{P}_{ij}$, which is proportional to $a_i^4 |\gamma\lambda^2 - 1|$, is typically much larger than unity for particle radii larger than 1 μm except when the i-particle and j-particle

considered are nearly identical ($\lambda \approx 1$, $\gamma \approx 1$). In this case, the Brownian motion must be taken into account. Thus the value of S_{ij}, when $\lambda \approx 1$ and $\gamma \approx 1$, cannot be directly obtained by extrapolating the theoretical results given in tables 1 and 2, which assume large Péclet numbers (i.e. negligible Brownian effect). But, extrapolating these known results out of their range of validity is the only way we have to estimate a coefficient S_{ii} that we can use, because the effective behaviour of the coefficient S_{ij} near the limit $\lambda = \gamma = 1$ remains unknown up to now.

In our experiments, almost all of the couples of nearly identical particles i and j ($\lambda \approx 1$, $\gamma \approx 1$) are such that $|\gamma - 1| \ll |\lambda - 1| \ll 1$. Consequently, the contribution of the few couples of particles for which $|\gamma - 1| \approx |\lambda - 1| \ll 1$ can be neglected. Therefore, the value of the coefficient S_{ii} that we must use to calculate U and S_t (30) and (31)) is $S_{ii} = -5.6$ (anyway, the contribution of S_{ii} to the weighted average of the theoretical sedimentation coefficient S_{ij}, namely S_t, would not be shifted by more than 0.1% if $S_{ii} = -5.6$ were replaced by $S_{ii} = -6.55$).

Consider now two particles i and j which differ from each other in density and size. One particle is made of silica and the other of magnesium; the histograms are shown in table 3. The values of γ and λ concerned are [$\gamma = 1.97$; $0.33 \leqslant \lambda \leqslant 0.87$] and $\gamma = 0.51$; $1.15 \leqslant \lambda \leqslant 3.02$]. For most of these values, permanent doublets of spheres may exist (Wacholder & Sather 1974) and the coefficient S_{ij} was not calculated by Batchelor & Wen (1982). The reason for this gap in the theory was presented in the introduction. Here we simply extrapolate Batchelor & Wen's results for S_{ij} out of their range of validity, in order to have an estimate of the theoretical average coefficient of sedimentation, namely S_t.

4. Results and discussion

Two sets of measurements are presented in this paper: one for a polydisperse suspension of silica spheres ($p_0 = 0$), with initial volume concentrations ϕ_0 in the range 0.0013–0.025 and the other one for a polydisperse suspension of both magnesium spheres and silica spheres in various volume proportions p_0 with a total volume concentration $\phi_0 = 0.02$. The experimental results for V (in fact V/U where U is the quantity calculated in (30)) as a function of the initial volume concentration $\phi_0(p_0 = 0)$ and as a function of the volume proportion $p_0(\phi_0 = 0.02)$, are respectively shown in figures 4 and 5 (dots) with their error bars; the continuous lines are the corresponding theoretical curves obtained from (29), (30) and (31); the crosses are the theoretical results corrected for the wall effects, as explained below.

The influence of the error on the measurement of the particle diameters appears in the experimental results for V/U because U (equation (30)) varies with a_i and in the same way for the theoretical results for V/U (equation (29)) because S_t (equation (31)) also varies with a_i. The effect of the error on the χ_i in these equations was estimated by recalculating U and S_t for different samplings of the same population, using the histograms presented in §2.2. The resulting variation in U was then found to be 0.1% and the variation in S_t was found to be much smaller. There may also be a systematic shift of all the a_i which is evaluated with the error on the average diameter of all particles (that is less than 0.4%). The resulting error on U is less than 0.8% and the one on S_t is negligible. Finally, the main error due to the measurement of the particle diameters is the one on experimental points. It is estimated to be less than 0.9%, that is a fraction of the error bars in figures 4 and 5.

For the first set of measurements (presented in figure 4), a linear regression analysis of the data has been carried out; the slope S_e (that is the experimental

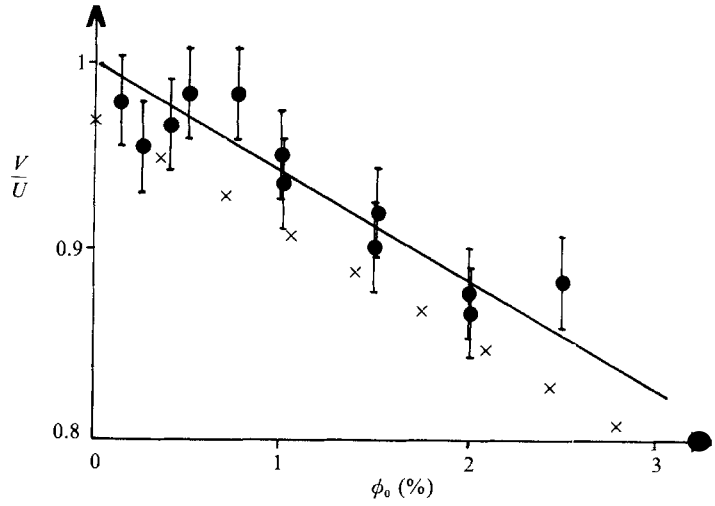

FIGURE 4. The dependence of V/U upon ϕ_0 for polydisperse suspensions of silica spheres ($p_0 = 0$): ●, experimental values; ——, theoretical values (equations (29), (30) and (31)); ×, theoretical values taking into account the wall effects (V^w/U, equations (A 9), (A 10) and (A 11)).

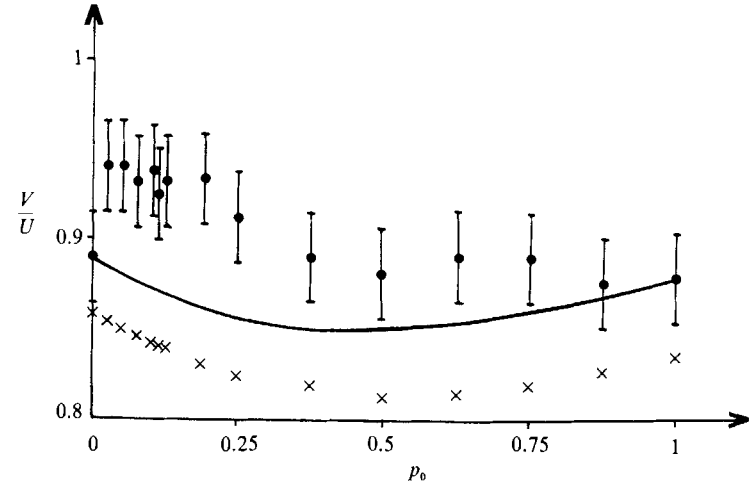

FIGURE 5. The dependence of V/U upon p_0 for polydisperse suspensions of silica spheres and magnesium spheres ($\phi_0 = 2\%$): ●, experimental values; ——, theoretical values (equations (29), (30) and (31)); ×, theoretical values taking into account the wall effects (V^w/U, equations (A9), (A 10) and (A 11)).

average coefficient of sedimentation) and the intercept value $\mathscr{I}_e$ with the V/U axis of the linear regression line have been calculated with their 90% confidence limits (see Bendat & Piersol 1971):

$$S_e = -5.3 \pm 1.1 \tag{32}$$

$$\mathscr{I}_e = 0.993 \pm 0.016. \tag{33}$$

We also calculated the standard deviation of the experimental values of V/U around the linear regression line with the slope $S_e = -5.3$ and we found 0.016. This suggests that the error bars (represented in figures 4 and 5) which were estimated from the experiments to be ± 0.025, were perhaps overestimated.

p_0	β_1	β_2
0	0.0300	−0.00009
0.025	0.0305	0.00031
0.05	0.0311	0.00063
0.075	0.0316	0.00088
0.1	0.0321	0.00108
0.112	0.0324	0.00116
0.125	0.0326	0.00122
0.1875	0.0340	0.00143
0.25	0.0352	0.00143
0.375	0.0377	0.00111
0.5	0.0402	0.00055
0.625	0.0426	−0.00007
0.75	0.0449	−0.00057
0.875	0.0472	−0.00078
1	0.0494	−0.00039

TABLE 4. Values of the wall effects coefficients β_1 and β_2 for different values of p_0.

We note that the intercept value $\mathscr{I}_e$ with the V/U axis is nearly equal to unity in (33); Stokes' law is apparently verified with high precision. However, this is not in fact true because of the wall effects and the temperature effects which will be discussed below. The possible influence of these factors on S_e will also be considered.

The theoretical value of the average coefficient of sedimentation (which is independent of ϕ_0) is for the set of silica particles

$$S_t = -5.60, \tag{34}$$

and thus our experimental average coefficient of sedimentation is in good agreement with the theoretical one. Measurements have been performed in suspensions of magnesium spheres with a total volume concentration in particles between 0.025% and 2.5%; the results we obtained for these suspensions confirm the agreement between the theory and the experiments for suspensions of particles which differ from each other in size.

Consider now the correction to the theoretical coefficient of sedimentation owing to the effects of the vertical walls of the cell. Geigenmüller & Mazur (1988) introduced terms for the averaged interactions between the walls and the particles; however, they did not calculate explicitly the direct wall effects on individual particles. We will now consider a simplified model for this effect. We consider first that the influence of a wall on the velocity of a sphere is independent of the influence of the other walls and second that the wall effects on the sedimentation coefficient S_{ij} are negligible; we show in the Appendix that, under such assumptions, the average velocity of sedimentation V^w in the homogeneous part of the suspension taking into account the effects of the cell walls can be approximately written as

$$V^w = U^w(1+S_t\phi_0), \tag{35}$$

where

$$U^w = U(1-\beta_1) \tag{36}$$

is an estimate of the modified weighted average Stokes velocity taking into account the wall effects (see β_1 in table 4). Thus, for $p_0 = 0$, the theoretical curve V^w/U as a function of ϕ_0 (crosses) is a straight line parallel to the straight line V/U as a function of ϕ_0 (continuous line) shown in figure 4. Then, according to this simplified model, by measuring the average velocity of sedimentation of a suspension in our cell, we

underestimate by an amount of about 3% the average velocity of sedimentation in an infinite suspension (that is the velocity calculated by Batchelor & Wen).

Geigenmüller & Mazur (1988) also showed theoretically that the presence of two vertical parallel plane walls modify the back flow in such a way that a large-scale convection may occur in the vessel. Using a condition of zero total flow across each horizontal plane, they showed that the mean volume flow profile between the two planes (which is symmetrical between the planes) is essentially a parabola with some adjustment next to the walls to fit with the no-slip condition of the fluid on these walls. The sedimentation is superimposed on this intrinsic convection of the fluid. In this model example, Geigenmüller & Mazur omit the direct wall effects on individual particles (that we estimated above). In our apparatus, the X-ray beam crosses the entire thickness of the cell and thus any convection due to the front and back walls, if it exists, is averaged out. On the other hand, there might be a sidewall effect, since the X-ray beam crosses only a fraction of the cell width: the 0.6 cm wide X-rays beam is centred in the 0.8 cm wide gap between the walls (the X-rays should not be tangent to the walls in order to avoid any fluorescence). Although Geigenmüller & Mazur (1988) only considered a monodisperse suspension, we can use their model to obtain an estimate of the effect of the intrinsic convection. We will assume for this purpose that the polydisperse suspension is equivalent to a monodisperse suspension with an average particle diameter. Using Geigenmüller & Mazur's figure 2, a simple integration over the parabolic profile for the mean volume flow (V_z in their notation) shows that the error induced by using the average flux over the middle (0.6 cm wide) part instead of over the whole (0.8 cm wide) gap is around 20% of the total variation of V_z between the parallel planes (which is $4.5\ \phi_0 U$). Since $\phi_0 \leqslant 2.5\%$ in the experiments, the error induced on the average sedimentation velocity V (averaged across the whole gap between the walls) is at most $0.2 \times 4.5 \times 0.025U = 0.02U$. In the centre of the gap, the mean volume flow is directed downwards (see Geigenmüller & Mazur's figure 2); thus, since the X-ray beam is located in the centre, the average sedimentation velocity V is over-estimated. In conclusion, the quantity V/U is over-estimated by 2%. This effect (if it exists) would tend to reduce the direct wall effects on individual particles that we estimated in (35) and (36).

Consider now the corrections due to the temperature. For a variety of reasons the experimental system does not allow us to measure the temperature very accurately and the systematic error we make on this quantity is estimated to be within ± 0.5 K: first, although the room in which our experiments are carried out is air-conditioned, a fluctuation of the temperature during each experiment is observed; secondly, the measurement of the temperature dependence of the fluid viscosity is carried out separately, with another thermometer. Furthermore, when we manipulate the fluid, an infinitesimal evaporation of the isopropanol may occur and thus the viscosity of the fluid may be slightly affected by this phenomenon. The average Stokes velocity U defined in (30) depends on the fluid viscosity η; thus, a possible underestimate of the temperature by 0.5 K produces as a consequence an overestimate of η, and therefore an underestimate of U by 2 or 3%. This possible underestimate of U does not affect the theoretical ratios V/U (where V is the theoretical velocity defined in (29)–(31)) and V^{w}/U (where V^{w} is the theoretical velocity defined in (35) and (36)); on the other hand, the overestimate of $1/U$ leads to an overestimate of the non-dimensional experimental velocity in figure 4. Finally the experimental points in figure 4 might be shifted by -0.03.

Consider now the corrections due to the wall effects together with the temperature effect: in figure 4, the continuous line may be translated down because of the wall

correction and the experimental points may be translated in the same direction because of a possible underestimate of the temperature. The compensation of these corrections may be one reason for the excellent value of the intercept $\mathscr{I}_e$ obtained in (33). It may also be that the corrections for the temperature and for the wall effects are overestimated. As far as the wall effects are concerned, (i) we have evaluated possible corrections for the direct interaction of walls and individual particles; (ii) we have estimated the possible error induced by the intrinsic convection (Geigenmüller & Mazur 1988) combined with the average over the width of the X-ray beam. These estimates are based on existing theories. However, there might be other effects, e.g. (iii) the interactions between each particle and a wall might be screened by the particles in between. An accurate theory for this effect still has to be formulated.

In conclusion, the theoretical and experimental coefficients of sedimentation (that is the slopes of the theoretical and experimental curves) are not modified by the corrections for the walls and the temperature. Thus the good agreement found between S_e and S_t (see (32) and (34)) is retained.

The second set of measurements concerns the mixture of magnesium and silica spheres in various volume proportions p_0 (between the values 0 and 1). Each dot in figure 5 corresponds to a measurement of the velocity of sedimentation for a given value of p_0. A single value of the total volume concentration, $\phi_0 = 0.02$, has been used. In figure 5, the continuous line represents the theoretical V/U from (29) and (30) and the crosses represent the theoretical V^w/U, where the superscript w stands for the wall effects calculated from our simplified model (see the Appendix and table 4). Note that the distance between the continuous line and the crosses does not remain constant. This is because the correction for the wall effects depends on a coefficient β_1 (see (36)) which depends on p_0 (see the Appendix and table 4). There is another possible effect of the walls, namely the intrinsic convection that we have considered above. Here again, we have to assume a monodisperse suspension in order to estimate this effect. The result of this convection effect is practically the same here, that is V/U is overestimated by about 2%. There is also, as with the first set of measurements, a possible correction for the temperature. Thus the experimental points could be shifted vertically. The good agreement in figure 5 between the dots (experimental results) and the solid line for $p_0 = 0$ and $p_0 = 1$ (i.e. for suspensions of one set of particles, as in figure 4) suggests that the walls and the temperature corrections either compensate or are overestimated, as pointed out earlier in the discussion of figure 4. Apart from the points $p_0 = 0$ and $p_0 = 1$, we observe a significant 6% deviation of the experimental points from the theoretical predictions on the average velocity of sedimentation. There is thus a large deviation (about 50%) from the theoretical predictions on the average coefficient of sedimentation. This deviation can be explained in the following way; among the coefficients S_{ij} which are introduced in the weighted average coefficient of sedimentation S_t (see (31)) for suspensions with both magnesium and silica particles ($p_0 \neq 0$ and $p_0 \neq 1$), some are obtained by extrapolating those available in table 1 and so, as we noted in § 1, are not strictly valid. The coefficients mentioned above do not take into account the fact that some of the relative trajectories of two particles i and j might be closed, that is some permanent doublets of particles may occur. Those close doublets have larger velocities than singlets. This may explain why the experimental average coefficient of sedimentation of the whole suspension is much larger than the one we obtained by calculation. In conclusion, this discrepancy between the (extrapolated) theory and the experiment may be experimental evidence of the existence of the permanent doublets.

5. Conclusion

An X-ray attenuation technique has been used to obtain the local concentration in spherical particles in polydisperse sedimenting suspensions as a function of vertical position and time. From these results, we determine the decrease with time of the total volume of particles above a given fixed horizontal plane. Then, by means of a time derivation, we obtain the average velocity of sedimentation in the interior homogeneous part of the suspension. This velocity can be compared to the ones obtained by Batchelor & Wen in homogeneous suspensions. This is a distinct improvement over earlier methods which follow the descent of the top front.

For suspensions of particles which differ in size only, the experimental coefficient of sedimentation is in good agreement with the theoretical one. For suspensions of particles which differ from each other both in size and density, the experimental settling factor has been compared to a theoretical one obtained by extrapolating Batchelor & Wen's results out of their range of validity. The fact that the experimental settling factor is significantly larger than the theoretical one may be evidence of the existence of permanent doublets of particles.

Finally, the accuracy of the measurements gives confidence in our experimental system. We now use our X-ray absorption technique to study the spreading of the top front for suspensions of particles which are polydisperse in sizes. The variation of the top front thickness with time is found to be larger than that predicted by accounting only for sphere polydispersity and hindered settling, as in Davis & Hassen's results (1988). This work is presently in progress.

We wish to thank Mme Liliane Chermant (ISMRA, Bd Maréchal Juin, Caen, France) for the determination of the diameter histograms, M François Bostel (Université de Rouen, France) for his technical contribution and Isabelle Fossey for the first experiments with suspensions of magnesium spheres. We also thank the referees for their constructive remarks and comments.

Appendix. An estimate of the wall effects

In order to estimate the wall effects on the average velocity of sedimentation in the homogeneous part of the settling suspension, we consider first the expression given by Lorentz (1897, 1907) of the force F_i exerted on a freely-rotating sphere of type i falling in isolation, parallel to one wall, in a viscous fluid with a velocity U_i

$$F_i = -6\pi a_i \eta \left(1 + \frac{9a_i}{16x}\right) U_i, \tag{A 1}$$

where x is the distance between the sphere's centre and the wall. Thus, considering that the influence of a wall on a sphere velocity is independent of the influence of the other walls, the balance of forces exerted on a sphere falling between two parallel walls at a distance l from each other leads to the sphere velocity

$$u_i = U_{i,0} \frac{1}{1 + \frac{9}{16} a_i \left(\frac{1}{x} + \frac{1}{l-x}\right)}. \tag{A 2}$$

We did not make use of the exact result given numerically by Ganatos, Pfeffer and Weinbaum (1980) for a sphere falling between two parallel vertical walls because the

much simpler approach chosen here is sufficient to evaluate the wall effects on U and S_t. Averaging then the velocity u_i (equation (A 2)) between $x = a_i$ and $x = l - a_i$ yields

$$U_i^{\mathrm{w}} = U_{i,0}\left(1 - \frac{9(D_i)^{\frac{1}{2}}}{8(D_i-2)\,(D_i+\frac{9}{4})^{\frac{1}{2}}} \ln \frac{((D_i(D_i+\frac{9}{4}))^{\frac{1}{2}}+D_i)-1}{((D_i(D_i+\frac{9}{4}))^{\frac{1}{2}}-D_i)+1}\right). \tag{A 3}$$

where the superscript w stands for the average wall effects. In the last equation, $D_i = l/a_i$ is a non-dimensional number with a value of the order of 10000 for the considered particle sets. Thus, expanding (A 3) for large values of D_i and neglecting the terms with orders greater than or equal to $1/D_i$, U_i^{w} can be approximated as follows:

$$U_i^{\mathrm{w}} = U_{i,0}(1-\epsilon_i), \tag{A 4}$$

where

$$\epsilon_i = \frac{9}{8}\frac{\ln D_i}{D_i}. \tag{A 5}$$

Bearing in mind that the X-ray beam crosses the entire thickness of the cell but not its entire width, only the cell's walls which are perpendicular to the X-ray beam have to be considered to estimate the wall effects on the average velocity of sedimentation in the homogeneous part of the settling suspension (nevertheless, taking into account the small effect of the two other vertical walls would be equivalent to multiplying ϵ_i by a factor much smaller than two). Thus, neglecting the wall effects on the sedimentation coefficients S_{ij}, the average velocity V_i^{w} of a test i-particle settling in the cell filled up with a homogeneous polydisperse suspension becomes

$$V_i^{\mathrm{w}} = U_i^{\mathrm{w}}\left(1 + \sum_{j=1}^{N} S_{ij}\,\phi_{j0}\right) = U_{i,0}(1-\epsilon_i)\left(1 + \sum_{j=1}^{N} S_{ij}\,\phi_{j0}\right). \tag{A 6}$$

Finally, letting

$$\beta_1 = \frac{\sum_{i=1}^{N} k_i\,\chi_{i0}\,a_i^2(\rho_i-\rho)\,\epsilon_i}{\sum_{i=1}^{N} k_i\,\chi_{i0}\,a_i^2(\rho_i-\rho)}, \tag{A 7}$$

and

$$\beta_2 = \frac{\sum_{i=1}^{N} k_i\,\chi_{i0}\,a_i^2(\rho_i-\rho)\,\epsilon_i \sum_{j=1}^{N} S_{ij}\,\chi_{j0}}{\sum_{i=1}^{N} k_i\,\chi_{i0}\,a_i^2(\rho_i-\rho) \sum_{j=1}^{N} S_{ij}\,\chi_{j0}} - \frac{\sum_{i=1}^{N} k_i\,\chi_{i0}\,a_i^2(\rho_i-\rho)\,\epsilon_i}{\sum_{i=1}^{N} k_i\,\chi_{i0}\,a_i^2(\rho_i-\rho)}, \tag{A 8}$$

where ϵ_i is defined in (A 5), the average velocity of sedimentation in the homogeneous part of the suspension, taking into account the wall effects in the cell, can be approximately written as follows

$$V^{\mathrm{w}} = U^{\mathrm{w}}(1 + S_{\mathrm{t}}^{\mathrm{w}}\,\phi_0), \tag{A 9}$$

where

$$U^{\mathrm{w}} = U(1-\beta_1), \tag{A 10}$$

and

$$S_{\mathrm{t}}^{\mathrm{w}} = S_{\mathrm{t}}(1-\beta_2), \tag{A 11}$$

neglecting terms with an order greater than $\ln D_i/D_i\,(i = 1, \ldots, N)$.

The values of β_1 and β_2 are given in table 4 for various values of p_0. We note that the effect of the coefficient β_2 (the absolute values of which are smaller than 0.00143) on $S_{\mathrm{t}}^{\mathrm{w}}$ is negligible when compared with the effect of the coefficient β_1 (the values of

which are greater than 0.0300) on U^w and, consequently, that $S_t^w \approx S_t$. Thus, although the Stokes velocities are present in the definition of the theoretical average coefficient of sedimentation (see (2) and (31)), this coefficient is not affected by the wall effects estimated here.

REFERENCES

Aïdi, M. 1986 Sur la sédimentation d'une suspension polydispersée homogène ou non. Thèse de docteur-ingénieur, Université de Rouen, France.

Aïdi, M., Feuillebois, F., Lasek, A., Anthore, R., Petipas, C. & Auvray, X. 1989 Mesure de la vitesse de sédimentation par absorption de rayons X. *Rev. Phys. Appl.* **24**, 1077–1084.

Anselmet, M. C., Anthore, R., Auvray, X., Petipas, C. & Blanc, R. 1989 Etude expérimentale de la sédimentation de particules sphériques. *C. R. Acad. Sci. Paris* **300** (2), 19.

Bacri, J. C., Frenois, C., Hoyos, M., Perzynski, R., Rakotomalala, N. & Salin, D. 1986 Acoustic study of suspension sedimentation. *Europhys. Lett.* **2** (2), 123–128.

Batchelor, G. K. 1972 Sedimentation in a dilute dispersion of spheres. *J. Fluid Mech.* **52**, 245–268.

Batchelor, G. K. 1982 Sedimentation in a dilute polydisperse system of interacting spheres. Part 1. General theory. *J. Fluid Mech.* **119**, 379–408.

Batchelor, G. K. & Wen, C.-S. 1982 Sedimentation in a dilute polydisperse system of interacting spheres. Part 2. Numerical results. *J. Fluid Mech.* **124**, 495–528. Corrigendum: *J. Fluid Mech.* **137**, 1983, 467–469.

Bendat, J. S. & Piersol, A. G. 1971 *Random Data: Analysis and Measurement Procedures*. Wiley Interscience.

Coster, M. & Chermant, L. 1989 Précis d'analyse d'images. Les Presses du CNRS – Normalisation Française de l'Afnor (X11–696, December 1989).

Davis, R. H. & Birdsell, K. H. 1988 Hindered settling of semidilute monodisperse and polydisperse suspensions. *AIChEJ.* **34**, 123–129.

Davis, R. H. & Hassen, M. A. 1988 Spreading of the interface at the top of a slightly polydisperse sedimenting suspension. *J. Fluid Mech.* **196**, 107–134.

Ganatos, P., Pfeffer, R. & Weinbaum, S. 1980 A strong interaction theory for the creeping motion of a sphere between plane parallel boundaries. Part 2. Parallel motion. *J. Fluid Mech.* **99**, 755–783.

Geigenmüller, U. & Mazur, P. 1988 Sedimentation of homogeneous suspensions in finite vessels. *J. Stat. Phys.* **53**, 137–173.

Ham, J. M. & Homsy, G. M. 1988 Hindered settling and hydrodynamic dispersion in quiescent sedimenting suspensions. *Intl J. Multiphase Flow* **14**, 533–546.

Klug, H. P. & Alexander, L. E. 1954 *X-ray Diffraction Procedure*, p. 92. John Wiley.

Kops-Werkhoven, M. M. & Fijnaut, H. M. 1981 Dynamic light scattering and sedimentation experiments on silica dispersions at finite concentrations. *J. Chem. Phys.* **74**, 1618.

Lorentz, H. A. 1897 A general theorem concerning the motion of a viscous fluid and a few consequences derived from it. *Verhand. Kon. Akad. Wet. Amst.* **5**, 168.

Lorentz, H. A. 1907 *Abh. über theor. Phys.* (Leipzig) **1**, 23.

Mirza, S. & Richardson, J. F. 1979 Sedimentation of suspensions of particles of two or more sizes. *Chem. Eng. Sci.* **34**, 447–454.

Stokes, G. G. 1851 On the effect of the internal friction of fluids on the motion of pendulums. *Trans. Camb. Phil. Soc.* **9**, 8.

Vasseur, P. & Cox, R. G. 1976 The lateral migration of a spherical particle in two-dimensional shear flows. *J. Fluid Mech.* **78**, 385–413.

Wacholder, E. & Sather, N. F. 1974 The hydrodynamic interaction of two unequal spheres moving under gravity through quiescent viscous fluid. *J. Fluid Mech.* **65**, 417–437.